Optimization of parameters of the excitation circuit of the traction synchronous generator

Dmitry Kornev

***Abstract* - In article proposed model of a synchronous generator designed for minimize losses in its excitation circuit. In the model, all generator loads are represented by functional dependencies on the design parameters of the machine and its magnetization characteristics. To determine the effect of the material of the magnetic core on the losses in the magnetic circuit, three types of electrical steel were taken into account: cast, sheet and steel grade 2212. The model takes into account the degree of saturation of the magnetic circuit of the machine, the reaction along the longitudinal and transverse axes at variable values of the electrical load and the main magnetic flux. The calculation of the magnetic circuit loads was carried out using the Blondel diagram in relative values.**

The dependences of the power of the excitation circuit of a synchronous generator are obtained in the possible range of changes in the design parameters and characteristics of the magnetization circuit. The factors that have the greatest influence on the efficiency of the excitation circuit of a synchronous generator are determined.

***Keywords* — electric drive, synchronous generator, optimization characteristics**

I. Introduction

The traction electric drive of locomotives consists of electric machines of ultimate use. The ultimate use machine involves working with the allowable maximal loads of all structural materials from which it is made. Such stringent requirements for traction machines are due to the requirements for their maximum efficiency and minimum dimensions, weight and power of auxiliary equipment.

II. Purpose of the Study

The most powerful machine in a traction electric drive is a synchronous generator of independent excitation (SG). On modern diesel locomotives, the power of traction generators reaches 4500 kW at a current in the power winding of 6000 - 8000 A.

The excitation winding circuit (EWG) of the SG generator is powered by an auxiliary electric machine - a single-phase synchronous generator B (exciter) - through a single-phase controlled rectifier bridge (Fig. 1).

Manuscript received Marth 11, 2023.
D. Kornev is with the Research and Design Institute for Information Technology, Signalling and Telecommunications in Railway Transportation (Jsc Niias), 109029, Nizhegorodskaya str.27, bldg. 1, Moscow, Russia (e-mail: da.kornev@gmail.com)

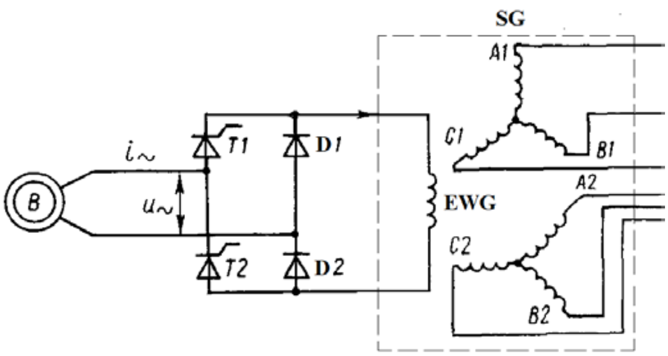

Fig.1. Scheme of the excitation winding circuit of the traction generator

The two arms of the bridge contain thyristors T1 and T2 (to control the current in the excitation winding of the EWG generator); the other two are diodes D1 and D2. To reduce the SG voltage ripple, its stator winding consists of two "stars" A1B1C1 and A2B2C2. The windings of the "stars" are shifted relative to each other by 30 electrical degrees.

Thus, the excitation winding circuit of the traction generator connects two electric machines, the SG and the V. Optimization of the parameters and operating mode of this circuit will increase the efficiency of the entire traction drive of the locomotive and reduce the cost of auxiliary systems.

III. Model of the Synchronous Generator of Independent Excitation

The SG model as an electromechanical object is a complex multifunctional system based on the properties of a magnetic circuit. (Fig. 2).

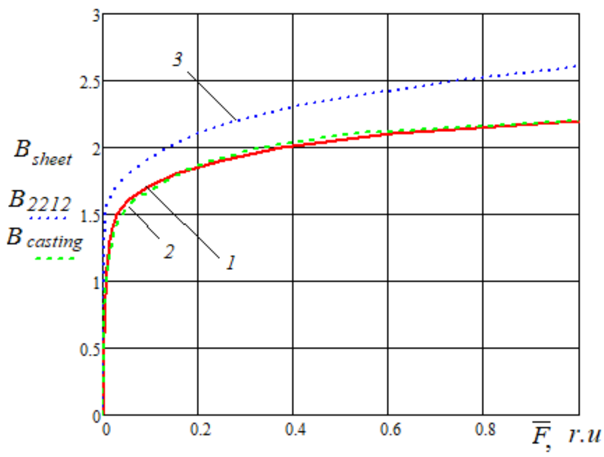

Fig. 2. Comparative characteristics of the magnetization of electrical steel: 1- electrical steel sheet; 2 - electrical steel casting; 3 - electrical steel grade 2212

The basis of the model is the magnetic circuit of the machine. It was assumed in the calculation that the SG magnetic circuit can be made from cast electrical steel, sheet electrical steel, and steel grade 2212.

The purpose of the calculation was to determine the design parameters of the machine, the control of which will minimize the losses of the SG magnetic circuit.

The initial data for the machine were power, line voltage and its frequency. These values for SG are normalized, since they determine the mechanical moment and speed of the traction drive. The system model was built taking into account the recommendations [1,2,3]. All design parameters of the machine were variable within the allowable range of changes and interconnected by functional dependencies on the design parameters of the machine and the characteristics of the magnetization of electrical steel in accordance with [1].

The model assumed a pole design in which the pole piece provides an approximately sinusoidal magnetic field in the air gap. As a rule, in synchronous machines, the ratio $\delta_{\text{M}}/_{\delta} \approx 1{,}5$, must be fulfilled for this, where δ_{M} is the air gap under the edge of the pole voltage [1,4].

This requirement is caused by the need to obtain a magnetic field in the air gap with a minimum number of higher harmonic components of the magnetic flux. If the magnetic field contains a large number of higher harmonic components, then losses will increase in the machine.

The magnetic circuit was considered as a single system that consists of a stator magnetic circuit, a rotor magnetic circuit and an air gap. Depending on the load of the machine, the value of the magnetic field will change. Under heavy load, the machine switches to the saturation mode of the magnetic circuit. This occurs in the tooth of the stator and the magnetic pole tips of the rotor. Therefore, for these areas, depending on the load, the magnetomotive force (MMF) of the tooth layer was calculated.

The losses of the magnetic circuit of the machine were determined by the MMF.

The MMF values were taken using the magnetization characteristics of the electrical steel from which the magnetic circuit was made.

The model of the magnetic circuit of the machine links the electrical and magnetic characteristics of the SG (1):

$$
\left\{
\begin{array}{c}
P_B(f_{\delta zc}, f_\delta, \delta, \tau, \alpha_p, b_{ch}, b_{z1}, q_{q1}) = U_1 \cdot I_B(f_{\delta zc}, f_\delta, \delta, \tau, \alpha_p, b_{ch}, b_{z1}, q_{q1}); \\
I_B(f_{\delta zc}, f_\delta, \delta, \tau, \alpha_p, b_{ch}, b_{z1}, q_{q1}) = \Delta_B(\delta, \tau, \alpha_p) \cdot s_B(f_{\delta zc}, f_\delta, \delta, \tau, \alpha_p, b_{ch}, b_{z1}, q_{q1}); \\
\Delta_B(\delta, \tau, \alpha_p) = 20\sqrt{\dfrac{\alpha_T[v_p(f,\delta)]k_T(\delta,\tau,\alpha_p)}{b(\delta,\tau,\alpha_p)}}\ ; \\
s_B(f_{\delta zc}, f_\delta, \delta, \tau, \alpha_p, b_{ch}, b_{z1}, q_{q1}) = \dfrac{\rho_m \cdot p \cdot F_{HB}(f_{\delta zc}, f_\delta, \delta, \tau, \alpha_p, b_{ch}, b_{z1}, q_{q1}) \cdot L_{Bcp}(\delta, \tau, \alpha_p)}{U_B}; \\
F_{HB}(f_{\delta zc}, f_\delta, \delta, \tau, \alpha_p, b_{ch}, b_{z1}, q_{q1}) = F_{rd}(f_{\delta zc}, f_\delta, \delta, \tau, \alpha_p, b_{ch}, b_{z1}, q_{q1}) + \\
F_{ad}(f_{\delta zc}, f_\delta, \delta, \tau, \alpha_p, b_{ch}, b_{z1}, q_{q1}) + F_m(f_{\delta zc}, f_\delta, \delta, \tau, \alpha_p, b_{ch}, b_{z1}, q_{q1}); \\
F_{rd}(f_{\delta zc}, f_\delta, \delta, \tau, \alpha_p, b_{ch}, b_{z1}, q_{q1}) = F[E_{rd}(f_{\delta zc}, f_\delta, \delta, \tau, \alpha_p, b_{ch}, b_{z1}, q_{q1})]; \qquad (1) \\
F_{ad}(f_{\delta zc}, f_\delta, \delta, \tau, \alpha_p, b_{ch}, b_{z1}, q_{q1}) = \\
\widetilde{\chi_d}\left(\dfrac{f_{\delta zc}}{f_\delta}\right) \cdot k_{ad}(\alpha_p) \cdot F_a(\delta, \tau, \alpha_p, b_{ch}, b_{z1}) \cdot sin\psi(f_{\delta zc}, f_\delta, \delta, \tau, \alpha_p, b_{ch}, b_{z1}, q_{q1}) + \\
\tilde{k}\left(\dfrac{f_{\delta zc}}{f_\delta}\right) \cdot \left(\dfrac{\tau}{\delta}\right) \cdot F_a(\delta, \tau, \alpha_p, b_{ch}, b_{z1}) \cdot cos\psi(f_{\delta zc}, f_\delta, \delta, \tau, \alpha_p, b_{ch}, b_{z1}, q_{q1}); \\
F_m(f_{\delta zc}, f_\delta, \delta, \tau, \alpha_p, b_{ch}, b_{z1}, q_{q1}) = F[\Phi_m(f_{\delta zc}, f_\delta, \delta, \tau, \alpha_p, b_{ch}, b_{z1}, q_{q1})]; \\
\Phi_m(f_{\delta zc}, f_\delta, \delta, \tau, \alpha_p, b_{ch}, b_{z1}, q_{q1}) = \Phi_{rd}(f_{\delta zc}, f_\delta, \delta, \tau, \alpha_p, b_{ch}, b_{z1}, q_{q1}) + \\
\Phi_\sigma(f_{\delta zc}, f_\delta, \delta, \tau, \alpha_p, b_{ch}, b_{z1}, q_{q1}); \\
F_a = 0{,}9 \cdot m_1 \dfrac{w_1 \cdot k_{\text{об1}} \cdot I_1}{p}; \\
\Phi_{rd}(f_{\delta zc}, f_\delta, \delta, \tau, \alpha_p, b_{ch}, b_{z1}, q_{q1}) = F'(f_{\delta zc}, f_\delta, \delta, \tau, \alpha_p, b_{ch}, b_{z1}, q_{q1}) \\
\Phi_\sigma(f_{\delta zc}, f_\delta, \delta, \tau, \alpha_p, b_{ch}, b_{z1}, q_{q1}) = F'(f_{\delta zc}, f_\delta, \delta, \tau, \alpha_p, b_{ch}, b_{z1}, q_{q1}) \\
L_{Bcp}(\delta, \tau, \alpha_p) = 2 \cdot \left[l_m(\delta, \tau, \alpha_p) + \pi \cdot b_m(\delta, \tau, \alpha_p) + 0.1b\left(l_m(\delta, \tau, \alpha_p)\right) + 2\delta_1\right]; \\
\Phi_{rd}(f_{\delta zc}, f_\delta, \delta, \tau, \alpha_p, b_{ch}, b_{z1}, q_{q1}) = \dfrac{E_{rd}(f_{\delta zc}, f_\delta, \delta, \tau, \alpha_p, b_{ch}, b_{z1}, q_{q1})}{4 \cdot k_B \cdot f \cdot k_0 \cdot w_B}\ ,
\end{array}
\right.
$$

where $P_B(f_{\delta zc}, f_\delta, \delta, \tau, \alpha_p, b_{ch}, b_{z1}, q_{q1})$ - losses of the SG excitation winding circuit;;
I_1 - phase current of the stator winding;
U_1 – voltage on the excitation winding of the SG;
$I_B(f_{\delta zc}, f_\delta, \delta, \tau, \alpha_p, b_{ch}, b_{z1}, q_{q1})$ - current of the SG excitation winding circuit;
$\Delta_B(\delta, \tau, \alpha_p)$ - current density in the excitation winding;
$s_B(f_{\delta zc}, f_\delta, \delta, \tau, \alpha_p, b_{ch}, b_{z1}, q_{q1})$ - section of the excitation winding conductor;
$\alpha_T[v_p(f, \delta)]$ – specific heat transfer coefficient from the excitation winding surface;
$k_T(\delta, \tau, \alpha_p)$ - coefficient of heat transfer from the surface of the excitation winding;
$F_{HB}(f_{\delta zc}, f_\delta, \delta, \tau, \alpha_p, b_{ch}, b_{z1}, q_{q1})$ – resulting MMF;
$L_{Bcp}(\delta, \tau, \alpha_p)$ - the length of the turn of the excitation winding;
$F_{rd}(f_{\delta zc}, f_\delta, \delta, \tau, \alpha_p, b_{ch}, b_{z1}, q_{q1})$ – longitudinal flow MMF in the air gap;
$E_{rd}(f_{\delta zc}, f_\delta, \delta, \tau, \alpha_p, b_{ch}, b_{z1}, q_{q1})$ – is the electromotive force (EMF) induced by the resulting longitudinal flow in the air gap;
$F_{ad}(f_{\delta zc}, f_\delta, \delta, \tau, \alpha_p, b_{ch}, b_{z1}, q_{q1})$ - MMF of the excitation winding along the longitudinal axis;
$F_{aq}(f_{\delta zc}, f_\delta, \delta, \tau, \alpha_p, b_{ch}, b_{z1}, q_{q1})$ - MMF of the excitation winding along the transverse axis;
$F_m(f_{\delta zc}, f_\delta, \delta, \tau, \alpha_p, b_{ch}, b_{z1}, q_{q1})$ - excitation winding MMF;
F_a – amplitude of the MMF of the armature winding;
$F[E_{rd}(f_{\delta zc}, f_\delta, \delta, \tau, \alpha_p, b_{ch}, b_{z1}, q_{q1})]$ – MMF value determined by the relative characteristic of steel
magnetization from the electromotive force from the resulting longitudinal flow in the air gap;
$F[\Phi_m(f_{\delta zc}, f_\delta, \delta, \tau, \alpha_p, b_{ch}, b_{z1}, q_{q1})]$ - MMF value determined by the relative steel magnetization characteristic for the electromotive force from the magnetic excitation flux;
$F'(f_{\delta zc}, f_\delta, \delta, \tau, \alpha_p, b_{ch}, b_{z1}, q_{q1})$ - MMF value determined by the relative steel magnetization characteristic from the relative values of the resulting magnetic flux in the air gap $\Phi_{rd}(f_{\delta zc}, f_\delta, \delta, \tau, \alpha_p, b_{ch}, b_{z1}, q_{q1})$ and magnetic flux of the field winding;
$\Phi_m(f_{\delta zc}, f_\delta, \delta, \tau, \alpha_p, b_{ch}, b_{z1}, q_{q1})$ – magnetic flux of the excitation winding;
$\Phi_{rd}(f_{\delta zc}, f_\delta, \delta, \tau, \alpha_p, b_{ch}, b_{z1}, q_{q1})$ - longitudinal flow in the air gap;
$\Phi_\sigma(f_{\delta zc}, f_\delta, \delta, \tau, \alpha_p, b_{ch}, b_{z1}, q_{q1})$ – pole scattering flux;
$\widetilde{\chi_d}\left(\frac{f_{\delta zc}}{f_\delta}\right)$, $k_{ad}(\alpha_p)$, $\tilde{k}\left(\frac{f_{\delta zc}}{f_\delta}\right)$ – coefficients that take into account the effect of saturation of the magnetic circuit on the longitudinal component of the armature winding MMF;
$\psi(f_{\delta zc}, f_\delta, \delta, \tau, \alpha_p, b_{ch}, b_{z1}, q_{q1})$ – is the shift angle between current I_1 and EMF $E_{rd}(f_{\delta zc}, f_\delta, \delta, \tau, \alpha_p, b_{ch}, b_{z1}, q_{q1})$ (fig. 3);
$L_{Bcp}(\delta, \tau, \alpha_p)$ - the length of the turn of the excitation winding;
$l_m(\delta, \tau, \alpha_p)$, $b_m(\delta, \tau, \alpha_p)$, $b\left(l_m(\delta, \tau, \alpha_p)\right)$ - length, width and radius of the pole core fillet;
δ_1 - is the thickness of the insulation between the core and the pole coil;
δ, τ, α_p - values of the air gap, pole division, pole arc, which are considered in the model as independent quantities (arguments) subject to change in the possible range of values;
$f_{\delta zc}, f_\delta$ – are the relative values of the magnetic stress in the tooth layer and the air gap;
f - voltage frequency in the phase of the stator winding;
w_B, w_1 – the number of turns of the field winding and the phase of the armature winding;
q_{q1} – number of turns per pole and phase of the stator winding
b_{ch}, b_{z1} - slot opening width and stator tooth width;
$k_{об1}$ - winding coefficient of the stator winding phase;
k_0 – winding coefficient for the first harmonic of the EMF;
k_B – is the shape factor of the field curve;
m_1,p – is the number of phases and pole pairs of the stator winding.

The traction synchronous generator is salient-pole machines with $p = 5$. The determination of the MMF of the field winding F_{HB} of a salient-pole machine in the operating mode under load is carried out using the vector diagram [1, 2]. In this study, the Blondel diagram was used to calculate the parameters of the magnetic circuit. The Blondel vector diagram uses the "method of two reactions", when the anchor MMF is decomposed into two components: longitudinal F_d и and transverse F_q (Fig. 3) (1):

$$\begin{cases} F_d = F_a sin\psi; \\ F_q = F_a cos\psi. \end{cases} \qquad (2)$$

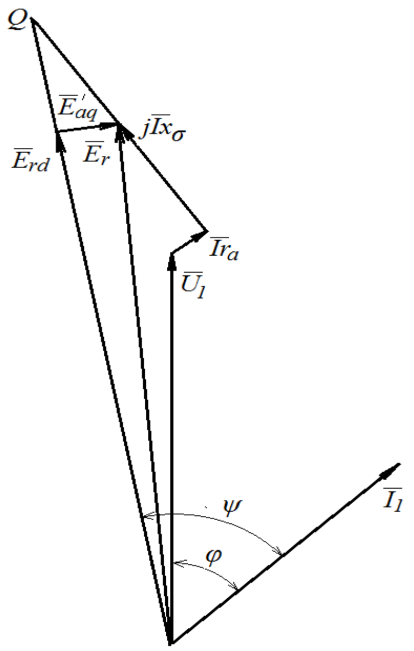

Fig. 3. Blondel diagram for the magnetic circuit of a traction synchronous generator

When the magnetic circuit of the machine is not saturated, the longitudinal component of the armature MMF F_d and the field winding MMF and the transverse armature MMF F_q act independently. In this case, the MMF of the armature winding can be represented as equivalent in terms of the action of the MMF of the excitation winding F_{ad} and F_{aq}. When calculating the Blondel diagram, it is assumed that the MMF of the excitation windings F_{ad} and F_{aq} are equivalent in terms of the action of the MMF of the armature windings F_d and F_q, if the first harmonic curves of the magnetic fields from F_d and F_q correspond to the first harmonic curves of the magnetic fields from F_{ad} and F_{aq}.

In order to pass to the values of F_{ad} and F_{aq} with known sinusoidally distributed F_d and F_q coefficients k_{ad} and k_{aq}. are used. These coefficients are determined by the distribution of the longitudinal and transverse components of the armature field and the excitation winding field in the air gap δ taking into account the geometry of the pole δ/τ and b_p/τ, where b_p- is the width of the pole piece

$$\begin{cases} F_{ad} = k_{ad} \cdot F_a sin\psi\,; \\ F_{aq} = k_{aq} \cdot F_a cos\psi\,. \end{cases} \tag{3}$$

When the machine is saturated, the longitudinal and transverse fields cannot be considered as independent. Therefore, the Richter method […] is used here, when the MMF of the resulting longitudinal and transverse components of the field are calculated taking into account the saturation of the magnetic circuit. The degree of saturation of the magnetic circuit is determined by the ratio $F_{\delta zc}/F_\delta$ and is taken into account by the nonlinear coefficients $\widetilde{\chi_d}\left(F_{\delta zc}/F_\delta\right)$ и $\widetilde{\chi_q}\left(F_{\delta zc}/F_\delta\right)$, where $F_{\delta zc}$- is the MMF of the tooth layer of the machine, F_δ - is the MMF in the air gap:

$$\begin{cases} F_{ad}' = \widetilde{\chi_d}\left(F_{\delta zc}/F_\delta\right) \cdot k_{ad} \cdot F_a sin\psi\,; \\ F_{aq}' = \widetilde{\chi_q}\left(F_{\delta zc}/F_\delta\right)\, k_{aq} \cdot F_a cos\psi\,. \end{cases} \tag{4}$$

Based on the relative magnetization curves of the machine, taking into account the values F_{aq}' (4) the relative value of the EMF from the transverse MMF E_{aq} is determined (Fig. 4).

The leakage flux of the magnetic circuit Φ_σ was calculated from the relative values of the longitudinal component MMF F_{ad}' and MMF from the resulting EMF $F_{rd}\left(f_{\delta zc}, f_\delta, \delta, \tau, \alpha_p, b_{ch}, b_{z1}, q_{q1}\right)$ (1).

The longitudinal component of the resulting magnetic flux in the air gap is determined by the value of the corresponding EMF [5] :

$$\Phi_{rd} = \frac{E_{rd}}{4k_B \cdot f \cdot k_o \cdot w_1}\,.$$

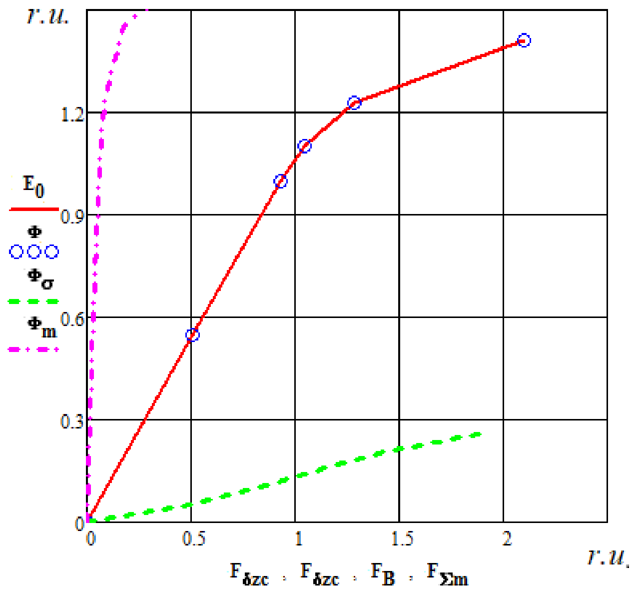

Fig. 4. Relative magnetization curves SG : $E_0, \Phi, \Phi_\sigma, \Phi_m$ - relative values of no-load EMF, no-load magnetic flux, leakage magnetic flux and field winding magnetic flux; $F_{\delta zc}, F_B, F_{\Sigma m}$ - relative values of the tooth layer MMF, MMF per pole pair, excitation winding MMF

According to the relative value Φ_{rd} according to the dependence (Fig. 4), the desired value of the magnetizing force of the excitation winding of a salient-pole synchronous machine under load is determined:

$$\begin{aligned} &F_{HB}\left(f_{\delta zc}, f_\delta, \delta, \tau, \alpha_p, b_{ch}, b_{z1}, q_{q1}\right) = \\ &F_{rd}\left(f_{\delta zc}, f_\delta, \delta, \tau, \alpha_p, b_{ch}, b_{z1}, q_{q1}\right) + \\ &F_{ad}\left(f_{\delta zc}, f_\delta, \delta, \tau, \alpha_p, b_{ch}, b_{z1}, q_{q1}\right) + \\ &F_m\left(f_{\delta zc}, f_\delta, \delta, \tau, \alpha_p, b_{ch}, b_{z1}, q_{q1}\right) \end{aligned}$$

.

The angle ψ, determined by the load angle of the machine, is calculated from the vector diagram (Fig. 3).

IV. Results of Research

The developed SG model makes it possible to identify the factors that most affect the losses in the magnetic circuit of the machine (Fig. 5). The calculation was carried out in relative values of the design parameters of the machine and the MMF of the magnetic circuit. The range of change was taken as follows:

- coefficient of the pole $\alpha_p = b_\Pi/\tau$ $0{,}7\ \text{o.e.} \le \overline{\alpha_p} \le 1{,}1\ \text{o.e}$, where b_Π – is the width of the pole piece;
- air gap $0{,}5\ \text{o.e} \le \bar{\delta} \le 1{,}2\ \text{o.e}$;
- stator winding tooth width $0{,}6\ \text{o.e.} \le \overline{b_{Z1}} \le 1{,}2\ \text{o.e}$;
- opening of the stator slot $0{,}6\ \text{o.e.} \le \overline{b_{ch1}} \le 1{,}2\ \text{o.e}$;
- MMF of the toothed layer $0{,}2\ \text{o.e.} \le \overline{f_{\delta zc}} \le 1{,}0\ \text{o.e}$.

As base values were taken $\alpha_p = 0{,}73$, $\delta = 0{,}0046\ mm$, $b_{Z1} = 0{,}0166\ mm$, $b_{ch1} = 0{,}0152\ mm$, $f_{\delta zc} = 1{,}015\ \text{o.e.}$ were taken as base values. (for electrical steel grade 2212).

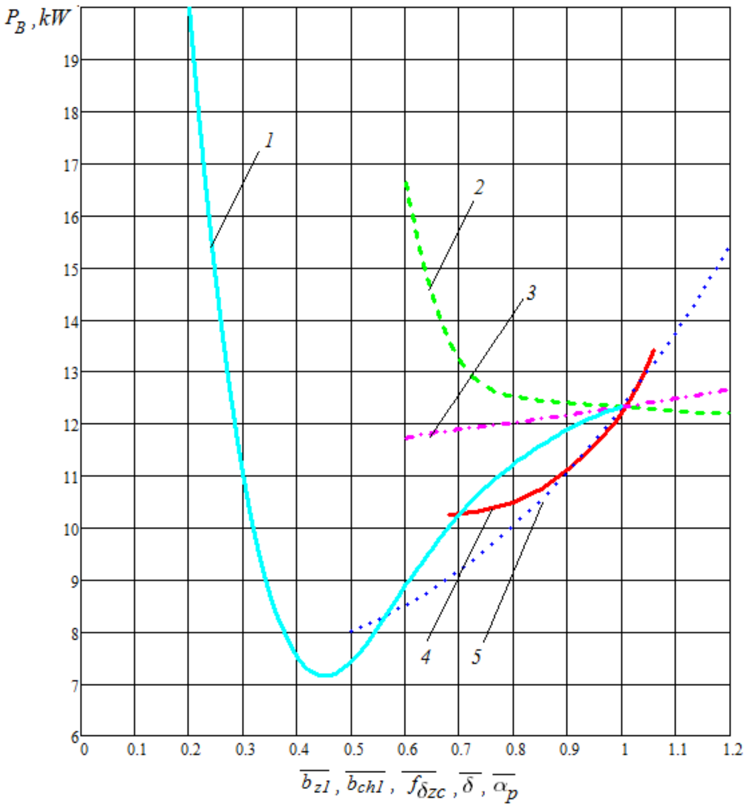

Fig. 5. Losses in the magnetic circuit of a synchronous generator on the relative values of design parameters: 1 – losses depending on the grade of electrical steel $\overline{f_{\delta zc}}$ (the magnetic characteristic of steels was taken as a continuous value depending on the grade of steel according to Fig. 2); 2 – losses depending on the value $\overline{b_{Z1}}$; – losses depending on the value $\overline{b_{ch1}}$; 4 – losses depending on the value $\overline{\alpha_p}$; 5 – losses depending on the value of $\bar{\delta}$

V. Conclusions

As a result of the calculations performed, it was found that the losses in the magnetic circuit of the SG are most affected by the material of the magnetic circuit (grade of electrical steel), the height of the air gap under the axis of the pole $\bar{\delta}$ and the width of the tooth of the stator magnetic circuit $\overline{b_{Z1}}$.

As can be seen from fig. 5 for the obtained dependencies, you can get a common extremum by folding the optimization criteria $\overline{b_{Z1}}$, $\overline{b_{ch1}}$, $\overline{\alpha_p}$, $\bar{\delta}$, $\overline{f_{\delta zc}}$ into an objective function. However, the solution of this problem requires the calculation of restrictions on the values $\overline{b_{Z1}}$, $\overline{b_{ch1}}$, $\overline{\alpha_p}$, $\bar{\delta}$, $\overline{f_{\delta zc}}$ taking into account the operating modes of the SG, the permissible size, current density in the conductors of the stator and rotor windings (depending on the type of machine cooling), etc. The dependencies shown in fig. 5, only the magnetic circuit of the machine is examined at constant values of current and voltage in the SG stator winding.

But even this study shows that it is possible to reduce the power of the excitation winding circuit of the SG by 2 times by optimizing the parameters of the machine and using modern grades of sheet electrical steel.

References

[1] Sergeev P.S. *Proektirovanie elektricheskih mashin* / P.S. Sergeev, N.V. Vinogradov, F.A. Goryanonov – 3-e izd., pererab. i dop. – M.: Energya, 1969. – 632 s. (in Russian)

[2] B. Marcusson and U. Lundin, *"Axial magnetic fields, axial force, and losses in the stator core and clamping structure of a synchronous generator with axially displaced stator,"* Electric Power Components and Systems, vol. 45 2017, no. 4, pp. 410–419,

[3] S.A. Gandzha, *Variable speed power* / S.A. Gandzha, I.E. Kiessh //Procedia Engineering. – 2015. – Vol. 129. – pp. 731–735.DOI:10.1016/j.proeng.2015.12.095

[4] S.A. Gandzha, A. Kotov, N. Neustroev, *Geometry Optimization of Asynchronous Synchronous Alternator with Using Generalized Variables* // 2019 International Ural Conference on Electrical Power Engineerings (UralCon). –2019. – pp. 373–377. DOI: 10.1109/URALCON.2019.8877634.

[5] Salynov S.A., Goryaev V.M. *Ocenka rascheta sinhronnogo generatora*, Kalmycki Ujsydarstvenny yniversitet imeni B.B. Geredikova – Available: https://s.econf.rae.ru/pdf/2017/12/6717.pdf (in Russian)